

Vortex glass transition in a random pinning model

Anders Vestergren^(a), Jack Lidmar^(b), and Mats Wallin^(a)

(a) Condensed Matter Theory, Royal Institute of Technology, SCFAB, SE-106 91 Stockholm, Sweden

(b) Department of Physics, Stockholm University, SCFAB, SE-106 91 Stockholm, Sweden

We study the vortex glass transition in disordered high temperature superconductors using Monte Carlo simulations. We use a random pinning model with strong point-correlated quenched disorder, a net applied magnetic field, longrange vortex interactions, and periodic boundary conditions. From a finite size scaling study of the helicity modulus, the RMS current, and the resistivity, we obtain critical exponents at the phase transition. The new exponents differ substantially from those of the gauge glass model, but are close to those of the pure three-dimensional XY model.

PACS numbers: 74.60.-w, 05.70.Fh, 75.40.Mg

The magnetic field-temperature phase diagram for vortices in disordered high temperature superconductors has been the focus of considerable interest in the past few years, centered around e.g. the suggestion of M. P. A. Fisher of a possible vortex glass phase with vanishing linear resistance [1]. Numerical simulation is often an important tool in investigations of phase transitions in vortex systems. For example, recent simulations have provided valuable information about the phase diagram for the case of weak disorder or weak magnetic fields [2]. Here evidence for a first order transition separating a Bragg glass phase [3], i.e. a dislocation-free solid with algebraically decaying translational order, from a vortex liquid phase was obtained. However, in the opposite limit of strong disorder or strong magnetic fields, the existence of a vortex glass phase, i.e. a vortex solid which is topologically disordered in terms of frozen in dislocations, and the critical properties of the vortex glass transition, have not been settled. In this paper we study these issues by Monte Carlo simulations and finite size scaling.

Simulations of disordered superconductors have often used a so-called gauge glass model [4], where the disorder is modeled as a random vector potential added to the phase difference of the superconducting order parameter. This disorder corresponds to spatially random magnetic flux present in the system. Interestingly, recent simulation results for the gauge glass [4] gives similar values for the critical exponents as obtained in certain recent experiments where a vortex glass has been reported [5]. However, the gauge glass model has two features that are not particularly realistic, namely, it does not assume any pinning directly affecting the vortex core energy, and, secondly, it is completely isotropic and does not contain any net magnetic field. It is at present unknown if these details are important for the universality class of the glass transition, i.e. if they modify the critical exponents. In particular, there is a possibility of anisotropic scaling produced by the net field, such that the correlation length diverges with different exponents along and perpendicular to the field. Some of these and other issues have been addressed in the literature.

An XY model with a random coupling constant and a

net magnetic field has been simulated using open boundary conditions [6]. However, periodic boundary conditions are preferable when bulk properties are studied, to avoid any influence of the sample surface. Also the effect of screening of the vortex interaction has been considered. Gauge field fluctuations lead to screening of the vortex interaction. This screening is usually rather weak in the high temperature superconductors. In models for the strong screening limit, simulations give evidence for the absence of a vortex glass phase at finite temperatures [7]. A vortex glass scenario without any thermodynamic phase transition has also been suggested [8].

In this paper we consider a random pinning model that contains all the pieces necessary to describe the static universal critical properties of the vortex glass critical point: long-range vortex interactions, strong vortex pinning, a net applied magnetic field, and periodic boundary conditions. The vortex-vortex interaction is a full 3D longrange interaction without screening, that becomes applicable when the bare screening length is much longer than the vortex spacing, i.e. in the strong field limit. The vortex pinning corresponds to uncorrelated quenched point disorder, implemented as a position dependent core energy. This is equivalent to random- T_c disorder. The vortex-vortex interaction and the disorder are isotropic in the model, but the applied net magnetic field breaks the spatial symmetry. We include the possibility of anisotropic scaling by allowing for different correlation length exponents in the directions parallel and perpendicular to the magnetic field. The dynamic universality class assumed here is that of relaxation dynamics of the vortex lines, and we stress that there are more dynamic universality classes possible [9].

The random pinning model is defined by the Hamiltonian

$$H = \frac{1}{2} \sum_{\mathbf{r}, \mathbf{r}'} V(\mathbf{r} - \mathbf{r}') \mathbf{q}(\mathbf{r}) \cdot \mathbf{q}(\mathbf{r}') + \frac{1}{2} \sum_{\mathbf{r}, \mu} D_\mu(\mathbf{r}) q_\mu(\mathbf{r})^2 \quad (1)$$

The model is defined on a simple cubic lattice with $\Omega = L \times L \times L_z$ sites, using periodic boundary conditions in all three directions. The vortex line variables are specified by an integer vector field $\mathbf{q}(\mathbf{r})$, whose $\mu = x, y, z$

component is the vorticity on the link from \mathbf{r} to $\mathbf{r} + \mathbf{e}_\mu$. The partition function is $Z = \text{Tr} \exp(-H/T)$, where T is the temperature, and Tr denotes the sum over all possible integers q_μ , subject to the constraint $\nabla \cdot \mathbf{q} = 0$ on all sites, i.e., the vortex lines have no open ends. An applied net magnetic field is included as a fixed number of vortex lines penetrating the system in the z -direction. Three different fillings of the applied magnetic field are considered here, i.e., number of vortex lines per link in the z -direction: $f = 1/2, 1/4, 1/\sqrt{10}$. For the irrational filling we used the integer number of vortex lines closest to fL^2 . The figures below are for $f = 1/2$. The long range vortex-vortex interaction is given by

$$V(\mathbf{r}) = \frac{K}{\Omega} \sum_{\mathbf{k}} \frac{e^{i\mathbf{k}\cdot\mathbf{r}}}{\sum_{\mu} (2 - 2 \cos k_{\mu})} \quad (2)$$

where $K = 4\pi^2 J$ (we set $J = 1$). On each link in the system is a short-range point-correlated random pinning energy with a uniform distribution in the interval $0 \leq D_\mu(\mathbf{r}) \leq K$. Hence the lattice constant of the discretization lattice in our model corresponds physically to a characteristic length scale for variations in the disorder energy landscape.

The Monte Carlo (MC) trial moves are attempts to insert vortex loops with random orientation on randomly selected plaquettes of the lattice. A MC sweep consists of one attempt on average to insert a loop on every plaquette. The attempts are accepted with probability $1/(1 + \exp \Delta E/T)$, where ΔE is the energy change for inserting the loop. For half and quarter fillings the initial vortex configurations consist of straight lines along the z -direction, arranged in a regular lattice in the xy -plane. For filling $f = 1/\sqrt{10}$ the initial configuration has straight lines placed at random. For equilibration about 10^5 MC sweeps are used, followed by equally many sweeps for collecting data. The results were averaged over up to 2000 samples of the disorder. Thermal averages are denoted by $\langle \dots \rangle$ and disorder averages by $[\dots]$. To avoid systematic errors in the calculation of squares of expectation values, two replicas of the system with the same disorder are used.

Superconducting coherence in the vortex line system can be detected by calculating the helicity modulus. One way of doing this [10] is to add a term $H_Q = \frac{K}{2\Omega} \mathbf{Q}^2$ to the Hamiltonian, where Q_μ is the total projected area of vortex loops added during the simulation. The helicity modulus in the direction μ is then given by

$$Y_\mu = 1 - \frac{K}{\Omega T} [\langle Q_\mu^2 \rangle - \langle Q_\mu \rangle^2] \quad (3)$$

and the RMS current density is defined as $J_\mu = \frac{K}{\Omega} [\langle Q_\mu^2 \rangle]^{1/2}$. The linear resistivity, ρ , is obtained from the Kubo formula for the resistance: [11]

$$R_\mu = \frac{1}{2T} \sum_{t=-t_0}^{t_0} [\langle V_\mu(t) V_\mu(0) \rangle] \quad (4)$$

where t is MC time, and the voltage is $V_\mu \propto \Delta Q_\mu$ is the net change in the projected vortex loop area during a sweep. In the calculation of ρ the H_Q term is not included in H . The summation time t_0 is chosen large enough that the resistivity is independent of t_0 , but much shorter than the length of the simulation.

We use a generalization of the Fisher-Fisher-Huse [1] scaling ansatz to analyze our MC data. At the glass transition temperature T_c the correlation length in the xy -planes, ξ , and in the z -direction, ξ_z , and the correlation time, τ , are assumed to diverge as $\xi \sim |T - T_c|^{-\nu}$, $\xi_z \sim \xi^\zeta$, and $\tau \sim \xi^z$. The anisotropic finite size scaling ansatz [12] for the helicity modulus is

$$Y_x = L^{3-d-\zeta} f_x(L^{1/\nu}(T - T_c), L_z/L^\zeta) \quad (5)$$

$$Y_z = L^{1-d+\zeta} f_z(L^{1/\nu}(T - T_c), L_z/L^\zeta), \quad (6)$$

where $d = 3$ is the spatial dimensionality and f_μ are scaling functions (scaling functions will from now on be suppressed in the equations). The current density scales as $J_x \sim L^{2-d-\zeta}$, $J_z \sim L^{1-d}$. The linear resistivity $\rho = E/J$, where E is the electric field, obeys

$$\rho_x \sim L^{d-3+\zeta-z}, \rho_z \sim L^{d-1-\zeta-z}, \quad (7)$$

We did a number of tests of equilibration of our simulations. We followed the standard procedure of calculating the ‘‘Hamming distance’’ between two replicas with identical disorders [13], for some selected system sizes L, L_z . We also increased the number of sweeps for equilibration with a factor of 10 for a few selected parameter values, and obtained no deviations from the data in the figures below. The linear resistivity (shown below in Fig. 4) gives an estimate of the relaxation time t_0 , which is the time where the curves saturate. The values for t_0 gives a rough estimate of the required equilibration time. The equilibration times used in our simulations are $\approx 8t_0$.

The first step is to verify that the model has a vortex glass phase, instead of a Bragg glass phase [3] that is expected for low fillings and weak disorder. Figure 1 shows a typical snapshot of a sample configuration for $T = 0.5 (\ll T_c)$, i.e. deep in the glass phase. This calculation was done using an exchange MC algorithm [14] with 9 uniformly spaced temperatures in $[0.5, 4.5]$. We also computed the structure function $S(\mathbf{q})$, and obtain no essential difference between S in the vortex liquid phase and the glass phase, with no indication of a Bragg glass phase [3]. This demonstrates that the low temperature phase of our model, for the filling and disorder strength considered, is indeed a glass where the vortex lines are frozen in random positions.

To locate the critical temperature of the vortex glass to liquid transition, ρ , and determine the critical exponents, MC data for the helicity modulus in the x and z directions is analyzed by the finite size scaling form in Eqs. (5),(6). MC data for different T, L, L_z for $f = 1/2$ is plotted in Fig. 2. To determine the anisotropy exponent

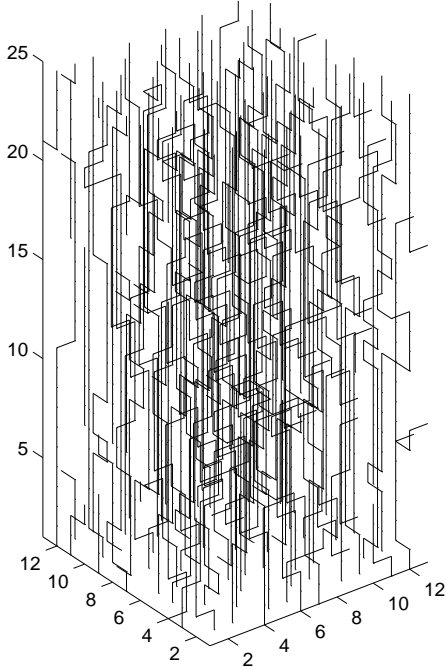


FIG. 1. Snapshot of a vortex line configuration from our MC simulation for $f = 1/2$ at $T = 0.5$ ($\ll T_c$) which is deep in the vortex glass phase.

ζ , a sequence of system sizes L_z are examined for each L . In the relation $L_z = cL^\zeta$, both c and ζ are varied until data curves for Y_x and Y_z for different system sizes $L = 6, 8, 10, 12$ become approximately independent of L at a common temperature, which is our estimate for T_c . Fig. 2 shows the best crossing obtained in this procedure, which gives $T_c = 4.5 \pm 0.1$, $\zeta = 1 \pm 0.1$. The same results are obtained from the RMS currents (inset). Equally good fits are obtained for c in the interval $1.5 < c < 2$. The errors are estimated as the interval outside which considerably poorer scaling is obtained.

To determine the correlation length exponent ν we use fits to Eqs. (5),(6) to obtain a data collapse for system sizes $L = 6 - 12$ over an entire temperature interval around T_c . As a measure of the quality of the collapse we define the RMS fit error $\Delta = \left[\sum_{L,T,\mu} (LY_\mu(L,T) - f_\mu(x))^2 \right]^{1/2}$, where $x = L^{1/\nu}(T - T_c)$, and f_μ is estimated by e.g. a cubic polynomial fit to the MC data. We did several different types of fits, all giving similar results. Figure 3 shows the best data collapse in a two parameter fit where both T_c and ν are varied independently in the x and z -directions. The best fit is obtained for $T_c = 4.5 \pm 0.1$, $\nu = 0.7 \pm 0.1$. A good data collapse is obtained, except for the smallest system size, where deviations are obtained below T_c . However for larger sizes scaling gets better, suggesting that the deviation for small system size is a finite size effect. The inset shows the RMS fit error as a function of ν

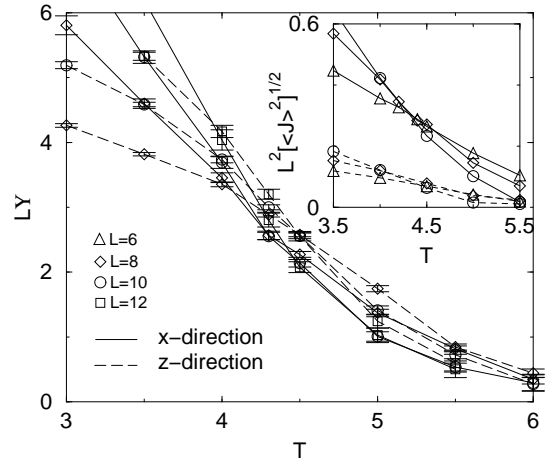


FIG. 2. MC data for the helicity modulus vs. temperature for different system sizes L . Inset: RMS current density vs. temperature.

for fixed $T_c = 4.5$. Nearly identical results are obtained by instead analyzing data for the RMS currents. The same result for ν is also obtained from an analysis of the derivative of the helicity moduli wrt T . For the lower fillings, $f = 1/4, 1/\sqrt{10}$, we find similar exponents but with larger error bars.

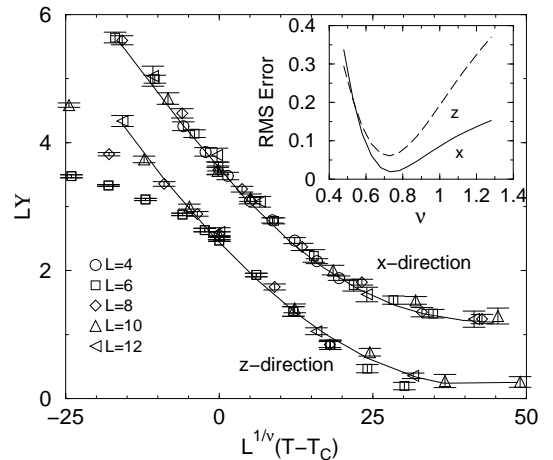


FIG. 3. Finite size scaling data collapse of MC data for the helicity moduli in the x and z -directions, obtained by fitting both T_c and ν . The data in the x -direction has been shifted to $LY_x + 1$ for clarity. Solid curves are guides to the eye. Inset: RMS fit error vs. ν at $T_c = 4.5$.

So far we have presented results for static quantities, and we now consider dynamics. The dynamic critical exponent is obtained from the linear resistivity in Eq. (4), for $f = 1/2$, $T = T_c = 4.5$, $L_z = 2L$. Fig. 4 shows finite size scaling data collapses according to Eq. (7) of MC data for ρ_x, ρ_z vs. the total MC integration time t_0 in the Kubo formula. The inset shows the RMS error in a power law fit to the MC data curves, and the best fit is obtained for $z = 1.5 \pm 0.2$. This gives a resistivity exponent in $\rho \sim t^s$ of $s = \nu(z - 1) \approx 0.3$.

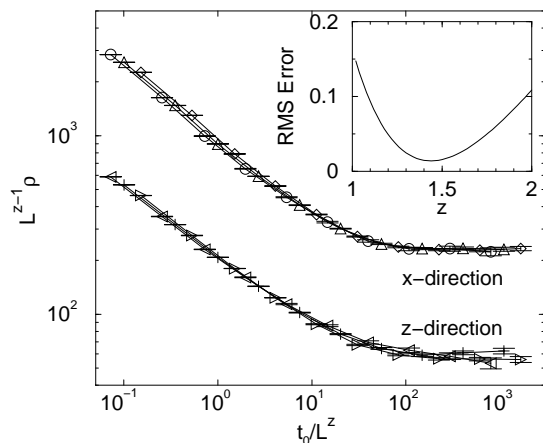


FIG. 4. Finite size scaling data collapse of MC data for the resistivity, obtained for $T_c = 4.5$, $z = 1.45$, and $L = 8, 10, 12$. Inset: RMS fit error in the data collapse.

We will now discuss the values obtained for the critical exponents of the random pinning model: $\zeta = 1 \pm 0.1$, $\nu = 0.7 \pm 0.1$, $z = 1.5 \pm 0.2$. Our correlation length exponent ν is close to the limiting value at a disordered fixed point allowed by the inequality [15]: $\nu \geq 2/d$. Within the precision obtained, we can not distinguish this exponent from that of the pure zero field 3D XY model, i.e. $\nu \approx 0.67$. Also our dynamic exponent $z \approx 1.5$ is consistent with the zero field 3D XY model with MC dynamics for vortex loops [16,9]. If confirmed, these results suggest a scenario where the vortex glass transition in the random pinning model for high fillings and strong disorder belongs to the zero field 3D XY universality class. In particular, this also suggests that the glass transition is driven by similar effectively isotropic, closed vortex loop fluctuations as in the zero field case, on top of a glassy groundstate.

Finally we compare our results with other models for the vortex glass transition and with experiments. The critical exponents obtained here for the random pinning model differ considerably from those of the gauge glass model [4]: $\nu \approx 1.39$, $z \approx 4.2$, $s = \nu(z - 1) \approx 4.5$, and also from a random coupling 3D XY model with an applied field and open boundary conditions [6]: $\nu \approx 2.2$, $z \approx 3.3$, $s \approx 5.3$. Hence, these models appear to belong to different universality classes than the random pinning model. Experiments on $(\text{K,Ba})\text{BiO}_3$ give $s \approx 3.9$, and experiments on untwinned proton irradiated $\text{YBa}_2\text{Cu}_3\text{O}_{7-\delta}$ give $s \approx 5.3$ [5]. These experiments show consistency with expected vortex glass behavior for tilting the magnetic field away from the c -axis. Unexpectedly, the exponents disagree considerably with our results. Further work is needed in order to clarify the reasons for this discrepancy.

In summary, we have observed a finite temperature continuous vortex glass transition by simulations and finite size scaling analysis of a three-dimensional ran-

dom pinning model. The critical exponents, $\zeta \approx 1$, $\nu \approx 0.7$, $z \approx 1.5$, are surprisingly close to those of the zero-field pure 3D XY model, but disagree with the gauge glass model and with some experiments. These results motivate further theoretical and experimental work.

We acknowledge very useful discussions with Pierre Le Doussal, Peter Olsson, Stephen Teitel, and Peter Young. This work was supported by the Swedish Natural Science Research Council, STINT, and PDC.

-
- [1] M. P. A. Fisher, Phys. Rev. Lett. **62**, 1415 (1989); D. S. Fisher, M. P. A. Fisher, and D. A. Huse, Phys. Rev. B **43**, 130 (1991).
 - [2] P. Olsson and S. Teitel, Phys. Rev. Lett. **87**, 137001 (2001). Y. Nonomura and X. Hu, Phys. Rev. Lett. **86**, 5140 (2001).
 - [3] T. Giamarchi and P. Le Doussal, Phys. Rev. Lett. **72**, 1530 (1994); Phys. Rev. B **55**, 6577 (1997).
 - [4] T. Olson and A. P. Young, Phys. Rev. B **61**, 12467 (2000).
 - [5] T. Klein, A. Conde-Gallardo, J. Marcus, C. Escribè-Filippini, P. Samuely, P. Szabó, and A. G. M. Jansen, Phys. Rev. B **58**, 12411 (1998). A. M. Petrean, L. M. Paulius, W.-K. Kwok, J. A. Fendrich, and G. W. Crabtree, Phys. Rev. Lett. **84**, 5852 (2000).
 - [6] H. Kawamura, J. Phys. Soc. Jpn. **69**, 29 (2000).
 - [7] H. S. Bokil and A. P. Young, Phys. Rev. Lett. **74**, 3021 (1995). J. Kisker and H. Rieger, Phys. Rev. B **58**, R8873 (1998).
 - [8] C. Reichhardt, A. van Otterlo, and G. T. Zimanyi, Phys. Rev. Lett. **84**, 1994 (2000).
 - [9] J. Lidmar, M. Wallin, C. Wengel, S. M. Girvin, and A. P. Young, Phys. Rev. B **58**, 2827 (1998).
 - [10] J. Lidmar and M. Wallin, Phys. Rev. B **59**, 8451 (1999).
 - [11] A. P. Young, Proceedings of the Ray Orbach Inauguration Symposium (World Scientific, Singapore, 1994).
 - [12] J. Lidmar and M. Wallin, Europhys. Lett. **47**, 494 (1999).
 - [13] M. Wallin, E. S. Sorensen, S. M. Girvin, and A. P. Young, Phys. Rev. B **49**, 12115 (1994).
 - [14] K. Hukushima and K. Nemoto, J. Phys. Soc. Jpn. **65**, 1604 (1996).
 - [15] A. B. Harris, J. Phys. C **7**, 1671 (1974). J. T. Chayes, L. Chayes, D. S. Fisher, and T. Spencer, Phys. Rev. Lett. **57**, 2999 (1986); Commun. Math. Phys. **120**, 501 (1989).
 - [16] H. Weber and H. J. Jensen, Phys. Rev. Lett. **78**, 2620 (1997).